Journal of Sound and Vibration 329 (2010) 56–71

Contents lists available at ScienceDirect

Journal of Sound and Vibration

journal homepage: www.elsevier.com/locate/jsvi

A versatile approach to the study of the transient response of a submerged thin shell

C. Leblond [a], J.-F. Sigrist [b,*]

[a] LEPTIAB, Université de la Rochelle, Pôle Science et Technologie, Avenue Michel Crépeau, 17042 La Rochelle Cedex 1, France
[b] DCNS Propulsion, Service Technique et Scientifique, 44620 La Montagne, France

ARTICLE INFO

Article history:
Received 26 January 2009
Received in revised form
23 August 2009
Accepted 24 August 2009
Handling Editor: C.L. Morfey
Available online 20 September 2009

ABSTRACT

The transient response of submerged two-dimensional thin shell subjected to weak acoustical or mechanical excitations is addressed in this paper. The proposed approach is first exposed in a detailed manner: it is based on Laplace transform in time, *in vacuo* eigenvector expansion with time-dependent coefficients for the structural dynamics and boundary-integral formulation for the fluid. The projection of the fluid pressure on the *in vacuo* eigenvectors leads to a fully coupled system involving the modal time-dependent displacement coefficients, which are the problem unknowns. They are simply determined by matrix inversion in the Laplace domain. Application of the method to the response of a two-dimensional immersed shell to a weak acoustical excitation is then exposed: the proposed test-case corresponds to the design of immersed structures subjected to underwater explosions, which is of paramount importance in naval shipbuilding. Comparison of a numerical calculation based on the proposed approach with an analytical solution is exposed; versatility of the method is also highlighted by referring to "classical" FEM/FEM or FEM/BEM simulations. As a conspicuous feature of the method, calculation of the fluid response functions corresponding to a given geometry has to be performed once, allowing various simulations for different material properties of the structure, as well as for various excitations on the structure. This versatile approach can therefore be efficiently and extensively used for design purposes.

1. Introduction

The development of efficient numerical methods to the study of large coupled transient problems remains a challenging subject, even in the linear regime and despite constantly improving computer capabilities. The behavior of submerged structures to weak acoustical or mechanical excitations belongs to this problems family, since in a first modeling step, the fluid medium is usually assumed acoustic, and the structural response of small-amplitude and elastic. In the design process of submarines or new underwater vehicles for military purposes, numerous simulations must be performed to minimize their transient responses to underwater explosion [1–3]. The shell width and material or the solicitation characteristics and location have to be changed to appreciate various configurations. Hence a method that allows not to repeat the whole numerical calculus for each particular case is of interest.

Such methods are available for simple geometries. More precisely, when the body shape conforms to a coordinate system in which the acoustic wave equation is separable, exact analytical response functions for the fluid are available in the time or frequency domains. They can then be used to model the fluid forces on each Fourier or structural modes [4].

* Corresponding author. Tel.: +33 2 40 84 87 84.
E-mail address: jean-francois.sigrist@dcnsgroup.com (J.-F. Sigrist).

0022-460X/$ - see front matter © 2009 Elsevier Ltd. All rights reserved.
doi:10.1016/j.jsv.2009.08.024

Hence, the response of simple submerged structures to a particular solicitation can be efficiently and rapidly obtained. For instance, the interaction problem between a shock wave and cylindrical shells configurations are achieved this way by Huang and Wang [5–8] and Iakovlev [9–14]. The three-dimensional problem involving a shock wave and a spherical shell has also attracted some attention and is tackled in [15,16]. These analytical or semi-analytical models are still extensively used in industrial applications to gain insight into complex fluid–structure interaction problems, to obtain the structural response order of magnitude, or in the validation process of numerical and approximate methods [17,18].

For complex geometries, exact analytical response functions for the fluid are not available. Hence numerical methods have been developed to tackle the fluid–structure interaction problem of the type considered. While finite element methods (FEM) are commonly used for the solid domain modeling, several choices can be made for the acoustic problem. FEM are of course appropriate but the coupling procedure become prohibitive in a design step since an infinite fluid domain has to be represented. Specific numerical procedures, such as infinite elements or artificial boundary conditions at the fluid domain edges, can be used to prevent waves reflections at the boundaries of the truncated domain [19]. However, finding such procedures that are both accurate for all frequencies and efficient for complex geometries is still a work-in-progress [20]. As alternative to the finite elements method for the fluid domain, boundary element methods (BEM) [21] based on integral formulations are really attractive, since the influence of the energy radiation to infinity is included in the fundamental solution [22]. Moreover, the method is particularly efficient for an infinite fluid domain, as only the fluid–structure interface has to be meshed, which reduces the problem dimension by one.

The first numerical coupling between the retarded potential equation—the classical integral formulation for a three-dimensional acoustic domain—and a finite elements method for the structure is attributed to Huang et al. [23]. Two difficulties are encountered. The first one is linked to storage requirement: the integral formulation is non-local in space and time, so the temporal evolution has to be stored at each interface node, and the amount of data necessary to integrate the equations of motion linearly increases at each time step. The second difficulty is linked to the temporal scheme stability. The standard retarded potential formulation is unstable for time steps inferior to a critical value [24], preventing the method from being useful for shock wave–shell interaction problems, where small time-steps are required. Specific numerical procedures, for instance based on the Figueiredo formulation [25], reduce the standard formulation critical time step and hence widen the application field of coupled finite elements-retarded potential numerical scheme. However, it is still not enough for shock wave–shell interaction problems [26].

Restricting storage requirements and stability conditions lead to the development of approximation methods to the retarded potential formulation. Two limiting cases, namely the "early-time" (or high-frequency) response and the "late-time" (or low-frequency) response, have been modeled by employing the initial value and final-value theorems to the Laplace transform of the Kirchhoff's spherical acoustic integral equation [27]. The plane wave approximation was also investigated for early-time responses [28]. Doubly asymptotic approximations (DAA) [29–31] have been proven to be adequate for characterizing the acoustic radiation damping affecting the structural responses that are dominated by low-frequency components [32]. Moreover, due to their direct implementation with finite element techniques for the structure, these approximations are often used in industrial applications [33,34]. However, the DAA-based methods contain some drawbacks: they fail to satisfy the early-time consistency requirement [35,36] and suffer from both frequency distortions and inaccurate radiation damping in the intermediate frequency domain [26,37]. Serious doubts can hence be put on the solution accuracy for highly transient dynamics of long duration [38], making these approximate methods unable to treat the structural response to underwater explosion bubble [39].

Recently, Chappell et al. [40] tackled successfully the boundary element method instability problem by reformulating the integral equation in the time-domain, thanks to the well-known Burton and Miller approach in the frequency domain [41]. Although it is applied to a purely radiation problem, it appears to be promising for highly transient fluid–structure interaction problems and could bypass the use of DAA methods, when coupling with finite element for the structure. An alternative is proposed in this paper. The integral equation is formulated in the Laplace domain and is coupled with the *in vacuo* modal decomposition for the structural dynamics. Spurious resonances in the fluid problem are eliminated with the use of the so-called "CHIEF points method", which is of convenient use for engineering applications; details on the method can for instance be found in [42].

The resulting coupling procedure is as versatile as the classical analytical or semi-analytical methods once the response functions are evaluated: there is no need to perform the whole numerical calculus again when a parameter value is changing. Due to both its formulation in the Laplace domain and the use of the modal decomposition, it is also suitable for parallel processing, which makes it efficient enough to be used for design purposes.

The method is developed here in a two-dimensional framework. This makes sense in the design or pre-design process since the detailed geometry is not determined yet. At this step, it is therefore useful to rapidly appreciate the acoustic solicitation effects on a relatively simple two-dimensional shape, which would be for instance representative of a full system part. This framework is moreover particularly meaningful for the case of elongated structures, for which qualitative as well as quantitative features are captured by a two-dimensional approach, as demonstrated for circular cylindrical shells [12,13,43]. The proposed method can indeed be seen as a first modeling step towards the more general three-dimensional problem.

The paper is organized as follows: the classical two-dimensional thin shell equations and the *in vacuo* modal decomposition are recalled in Section 2 for the sake of completeness. In the third part, the boundary integral formulation for the fluid are introduced and the fluid force explicitly expressed. The fluid–structure interaction problem is solved in

Section 4. Last, the method is illustrated for the shock wave/submerged circular thin shell interaction problem. Some method improvements and extensions are proposed in the conclusion.

2. Structural dynamics

We consider a two-dimensional elastic shell of constant thickness h and arbitrary shape, submerged in an infinite fluid medium and subjected to a weak incident acoustic excitation. A schematic of the problem is shown in Fig. 1. The shell is assumed thin and composed of a linear, homogeneous and isotropic elastic material of density ρ_s. Under the Love–Kirchhoff hypothesis and neglecting the rotary inertia effects, the linear equations of motion for the shell can be written [44,45]:

$$\frac{\partial^2 \mathbf{X}}{\partial t^2}(\mathbf{x},t) + [L]\mathbf{X}(\mathbf{x},t) = \mathcal{K}(\mathbf{f}(\mathbf{x},t) - \mathbf{p}(\mathbf{x},t)). \tag{1}$$

The variables are normalized according to Table 1, with R a characteristic shell length, c_f the speed of sound in the fluid and ρ_f the fluid density. The quantity $\mathbf{X}(\mathbf{x},t) = (X_\alpha(\mathbf{x},t), X_\zeta(\mathbf{x},t))^{\mathrm{T}}$ denotes the dimensionless displacement vector at time t and position vector $\mathbf{x}(\alpha)$, with α the curvilinear coordinate of the shell. X_α and X_ζ are the tangential and normal in-plane displacements of the neutral surface of the shell, respectively. $[L]$ is the partial differential operator in space. The dimensionless number $\mathcal{K}$ is defined by $\mathcal{K} = \mathcal{M}/\mathcal{E}$, with $\mathcal{M} = \rho_f/\rho_s$ the density ratio and $\mathcal{E} = h/R$ the normalized shell thickness. The vector $\mathbf{f}$ corresponds to the force density term, representing a given mechanical excitation or induced by internal structures, and $\mathbf{p}$ represents the loading due to the surrounding fluid medium.

This fluid–structure interaction problem can be solved, without loss of generality, thanks to the *in vacuo* modal decomposition of the shell, since the corresponding eigenvectors form a complete set. The displacement vector of the submerged shell is therefore formulated as follows:

$$\mathbf{X}(\mathbf{x},t) = \sum_m d_m(t)\boldsymbol{\Phi}_\mathbf{m}(\mathbf{x}), \tag{2}$$

where $d_m(t)$ are the time-dependent modal displacement coefficients. The vectors $\boldsymbol{\Phi}_\mathbf{n}(\mathbf{x}) = (\Phi_n^\alpha(\mathbf{x}), \Phi_n^\zeta(\mathbf{x}))^{\mathrm{T}}$ represent the *in vacuo* eigenfunctions of the neutral surface of the shell, and satisfy the following eigenvalue problem and orthogonality property:

$$[L]\boldsymbol{\Phi}_\mathbf{n} = \Omega_n^2 \boldsymbol{\Phi}_\mathbf{n}, \tag{3}$$

$$\int_\Gamma \boldsymbol{\Phi}_\mathbf{n}^{\mathrm{T}}(\mathbf{x})\boldsymbol{\Phi}_\mathbf{m}(\mathbf{x})\,\mathrm{d}S_\mathbf{x} = \delta_{nm} M_n, \tag{4}$$

with Ω_n the eigenvalues and δ_{nm} the Kronecker symbol. Substitution of the modal decomposition, Eq. (2), for the displacement in Eq. (1), followed by the use of Eq. (3), multiplication of the resulting relation by $\boldsymbol{\Phi}_\mathbf{n}^{\mathrm{T}}$, and integration along the shell surface, yield the modal equation for the time-dependent displacement coefficient:

$$M_n \ddot{d}_n(t) + K_n d_n(t) = \mathcal{K}(f_n(t) - p_n(t)), \tag{5}$$

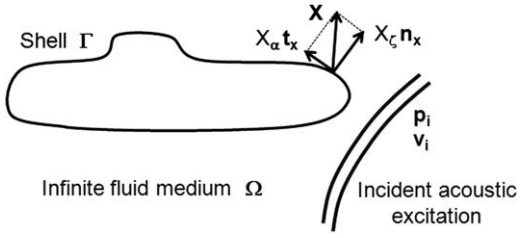

Fig. 1. Submerged two-dimensional thin shell subjected to an incident acoustic excitation.

Table 1
Normalization factors for the variables.

Variable	Normalization factor
Length	R
Time	R/c_f
Displacement	R
Velocity	c_f
Force density	$\rho_f c_f^2$
Pressure	$\rho_f c_f^2$

with K_n the modal stiffness given by $K_n = \Omega_n^2 M_n$. The term f_n represents the projection of the given mechanical excitation on the n th eigenfunction and the modal fluid force coefficient, p_n, is the fluid loading projection on the same quantity:

$$f_n(t) = \int_\Gamma \mathbf{\Phi}_\mathbf{n}^\mathrm{T}(\mathbf{x})\mathbf{f}(\mathbf{x},t)\,\mathrm{dS}_\mathbf{x}, \quad p_n(t) = \int_\Gamma \mathbf{\Phi}_\mathbf{n}^\mathrm{T}(\mathbf{x})\mathbf{p}(\mathbf{x},t)\,\mathrm{dS}_\mathbf{x}. \tag{6}$$

In order to solve each modal equation (5), the fluid force coefficient must be explicitly expressed as a function of the given acoustic excitation, the shell geometry and the time-dependent displacement coefficients. This is the purpose of the following section.

3. Fluid dynamics

3.1. The integral equation formulation

We consider a two-dimensional finite object, with regular boundary surface Γ, submerged in an infinite two-dimensional exterior acoustic field Ω, see Fig. 1. Ω is filled with a homogeneous compressible acoustic medium governed by the wave equation for the fluid pressure p. Assuming that the shell is subjected to small-amplitude motions and normalizing the variables according to Table 1, the fluid medium is governed by the initial-boundary value problem:

$$\left[\frac{\partial^2}{\partial t^2} - \nabla^2\right] p(\mathbf{x},t) = 0 \quad \text{in } \Omega \times \mathbb{R}_+, \tag{7}$$

$$p(\mathbf{x},0) = 0, \quad \dot{p}(\mathbf{x},0) = 0 \quad \text{in } \Omega, \tag{8}$$

$$\frac{\partial p}{\partial \mathbf{n}_\mathbf{x}}(\mathbf{x},t) = -\frac{\partial \mathbf{v}}{\partial t}(\mathbf{x},t)\mathbf{n}_\mathbf{x} \quad \text{on } \Gamma \times \mathbb{R}_+, \tag{9}$$

where $\mathbf{v}$ denotes the boundary velocity, initially at rest, and $\mathbf{n}_\mathbf{x}$ the outward unit normal vector to Γ at $\mathbf{x}$. Then, assuming that Γ is locally differentiable at $\mathbf{x}$, the fluid pressure on the boundary may be represented by the following integral equation [46,47]:

$$\frac{1}{2}p(\mathbf{x},t) = \mathcal{D}(p(\mathbf{x},t)) - \mathcal{S}\left(\frac{\partial p}{\partial \mathbf{n}_\mathbf{x}}(\mathbf{x},t)\right) \quad \text{on} \quad \Gamma \times \mathbb{R}_+, \tag{10}$$

where the single-layer and double-layer potentials, $\mathcal{S}$ and $\mathcal{D}$, are defined by

$$\mathcal{S}(\varphi(\mathbf{x},t)) = \int_0^{t^+}\int_\Gamma \mathcal{G}(\mathbf{x}-\mathbf{x}',t-\tau)\varphi(\mathbf{x}',\tau)\,\mathrm{dS}_{\mathbf{x}'}\,\mathrm{d}\tau, \tag{11}$$

$$\mathcal{D}(\varphi(\mathbf{x},t)) = \int_0^{t^+}\int_\Gamma \frac{\partial \mathcal{G}}{\partial \mathbf{n}_{\mathbf{x}'}}(\mathbf{x}-\mathbf{x}',t-\tau)\varphi(\mathbf{x}',\tau)\,\mathrm{dS}_{\mathbf{x}'}\,\mathrm{d}\tau, \tag{12}$$

In Eqs.(11) and (12), t^+ has to be understood as $t^+ = t + \varepsilon$ with ε arbitrarily small. The dimensionless fundamental solution of the two-dimensional wave equation is given by [48,49]

$$\mathcal{G}(\mathbf{x},t) = \frac{U(t-|\mathbf{x}|)}{2\pi\sqrt{t^2-|\mathbf{x}|^2}}, \tag{13}$$

with U the Heaviside function. Note that the integral equation (10) involves space-time integrals and is hence non-local in space and time. Contrary to the three-dimensional case, where the fundamental solution contains the term $\delta(t-|\mathbf{x}|)$ with δ the Dirac delta function, it cannot be reformulated with a surface integral only, like the well-known retarded potential integral equation. The integral equation is however linear and involves a temporal convolution product in $\mathbb{R}_+$, so employing the convolution theorem, it becomes local in the Laplace domain. Moreover, by using the boundary conditions Eq. (9), the integral equation can be written:

$$\frac{1}{2}\hat{p}(\mathbf{x},s) = \hat{\mathcal{D}}(\hat{p}(\mathbf{x},s)) + \hat{\mathcal{S}}(s\hat{\mathbf{v}}(\mathbf{x},s)\mathbf{n}_\mathbf{x}) \quad \text{on } \Gamma \times \mathcal{B}, \tag{14}$$

with s the Laplace variable belonging to the Bromwich contour $\mathcal{B}$. The Laplace transforms of the single and double-layer potentials take the form:

$$\hat{\mathcal{S}}(\hat{\varphi}(\mathbf{x},s)) = \int_\Gamma \frac{i}{4}H_0^{(1)}(is|\mathbf{x}-\mathbf{x}'|)\hat{\varphi}(\mathbf{x}',s)\,\mathrm{dS}_{\mathbf{x}'}, \tag{15}$$

$$\hat{\mathcal{D}}(\hat{\varphi}(\mathbf{x},s)) = \int_\Gamma -\frac{s}{4}H_1^{(1)}(is|\mathbf{x}-\mathbf{x}'|)\mathbf{e}_{\mathbf{x}\mathbf{x}'}\cdot\mathbf{n}_{\mathbf{x}'}\hat{\varphi}(\mathbf{x}',s)\,\mathrm{dS}_{\mathbf{x}'}, \tag{16}$$

where both the fundamental solution equation (13) and its normal derivative are written explicitly in the Laplace domain. The quantities $H_0^{(1)}$ and $H_1^{(1)}$ denote the Bessel functions of the third kind, also called the Hankel functions [50]. Eq. (16) is derived by using the following geometrical relation:

$$\frac{\partial|\mathbf{x}-\mathbf{x}'|}{\partial\mathbf{n}_{x'}} = -\mathbf{e}_{\mathbf{x}\mathbf{x}'}\cdot\mathbf{n}_{\mathbf{x}'} \quad \text{with } \mathbf{e}_{xx'} = \frac{\mathbf{x}-\mathbf{x}'}{|\mathbf{x}-\mathbf{x}'|}. \tag{17}$$

In accordance with the integral equation (14), the fluid pressure can symbolically be written as

$$\hat{p}(\mathbf{x},s) = \hat{\Pi}(\mathbf{x},s)s\hat{\mathbf{v}}(\mathbf{x},s)\mathbf{n}_{\mathbf{x}}, \quad \hat{\Pi}(\mathbf{x},s) = \left[1/2 - \hat{D}(\mathbf{x},s)\right]^{-1}\hat{S}(\mathbf{x},s), \tag{18}$$

where $\hat{S}(\mathbf{x},s)$ and $\hat{D}(\mathbf{x},s)$ result from the evaluation of the integral operators $\hat{\mathcal{S}}$ and $\hat{\mathcal{D}}$ respectively, achieved for instance by applying a boundary element method to Eqs. (15) and (16). Such a computation is realized for the particular case of a circular geometry in Section 5.

Some remarks have to be made here. One of the drawbacks frequently addressed in boundary elements methods in the frequency domain is that the surface Helmholtz integration fails to yield unique solutions at certain critical frequencies. They are known to be associated with the eigenfrequencies of the interior problem and do not represent any kind of physical resonance. At these frequencies, the integral operators are singular and become strongly ill-conditioned in their surroundings. As a consequence, the solution displays a non-physical behavior. Some methods, such as the Burton and Miller approach or the so-called "CHIEF point method" [41,42], are often employed to deal successively with these problems. Moreover, it is argued by Chappell et al. [40] that the integral formulation in the temporal domain implicitly contains these critical frequencies. Although they are not in itself a cause of instability, the loss of accuracy for the high frequencies due to the discretization leads to the deviation of the real part of the spurious eigenfrequencies in the right half-plane, which actually induces an unstable behavior, often observed when temporal schemes are used without the Burton and Miller approach.

In order to obtain the solution in the time domain, the integral operators are here first expressed in the Laplace domain. More precisely, they are evaluated on the Bromwich contour, i.e., on the line defined by $s = \sigma + \mathrm{i}\omega$ with σ fixed and strictly positive and ω varying in $]-\infty,+\infty[$. The integral operators are hence not evaluated on the imaginary axis, where the spurious eigenfrequencies lie, and are regular for all points of the Bromwich contour. However, they become ill-conditioned near those spurious eigenfrequencies, which may deteriorate the accuracy of the temporal solution.

That is the reason why the proposed approach is developed within the framework of the "CHIEF points method" for the BEM resolution of the fluid acoustic problem; this ensures that the influence of spurious frequencies on the numerical calculation remains negligible. Furthermore, the imaginary part of the Bromwich contour is limited, for numerical purpose, to a maximum value ω_{th}.

This means that the frequencies beyond ω_{th} are simply neglected, and not implicitly used as in the case of a temporal scheme. This prevents their wrong evaluations and deviations in the right half-plane, leading to the instability issues. These comments will be checked in Section 5, for the particular case of a shock wave/circular thin shell interaction problem. First of all, the symbolic equation (18) is exploited in the next section in order to explicitly express the modal fluid force coefficient, p_n, appearing in the modal equation (5).

3.2. Expression of the modal fluid force coefficients

By virtue of the acoustic problem linearity, the fluid pressure is classically divided into three components: p_i, p_d, and p_r. The incident pressure, p_i, is a given data, corresponding to the incident acoustic excitation and obtained without taking into account the submerged body. The second one, p_d, denotes the diffracted pressure by the body assumed fixed and rigid. It is introduced in order to balance the normal component of the incident wave velocity on the body surface, $\mathbf{v_i}\cdot\mathbf{n_x}$, which is also a given data. The last component, p_r, corresponds to the pressure radiated by the submerged body deformations. It is the only part coupled with the shell dynamics and should be expressed as a function of the modal displacement coefficients. The boundary conditions of the diffracted and radiated pressures on the shell surface are hence given by

$$\frac{\partial p_d}{\partial\mathbf{n_x}}(\mathbf{x},t) = \dot{\mathbf{v}}_{\mathbf{i}}(\mathbf{x},t)\mathbf{n}_{\mathbf{x}}, \quad \frac{\partial p_r}{\partial\mathbf{n_x}}(\mathbf{x},t) = -\ddot{\mathbf{X}}(\mathbf{x},t)\mathbf{n}_{\mathbf{x}}. \tag{19}$$

It is also useful to introduce the vectors $\mathbf{p_i}$, $\mathbf{p_d}$, and $\mathbf{p_r}$ such that only their normal components on the shell boundary are non-zero and given by p_i, p_d, and p_r, respectively. Hence the fluid loading appearing in the shell equation (1) can be written as $\mathbf{p} = \mathbf{p}_i + \mathbf{p}_d + \mathbf{p_r}$ and the modal fluid force coefficients defined by Eq. (6) take the form

$$p_n(t) = \int_\Gamma \mathbf{\Phi}_{\mathbf{n}}^{\mathrm{T}}(\mathbf{x})[\mathbf{p_i}(\mathbf{x},t) + \mathbf{p_d}(\mathbf{x},t) + \mathbf{p_r}(\mathbf{x},t)]\,\mathrm{d}S_{\mathbf{x}}. \tag{20}$$

Then performing a modal decomposition of the last two vectors such that

$$\mathbf{p}_d(\mathbf{x},t) = \sum_n p_d^n(t)\mathbf{\Phi_n}(\mathbf{x}), \quad p_d^n(t) = \frac{1}{M_n}\int_\Gamma \Phi_n^\zeta(\mathbf{x})p_d(\mathbf{x},t)\,\mathrm{d}S_{\mathbf{x}}, \tag{21}$$

$$\mathbf{p_r}(\mathbf{x},t)=\sum_n p_r^n(t)\mathbf{\Phi_n}(\mathbf{x}),\quad p_r^n(t)=\frac{1}{M_n}\int_\Gamma \Phi_n^\zeta(\mathbf{x})p_r(\mathbf{x},t)\,\mathrm{dS_x} \tag{22}$$

and using the orthogonality property, Eq. (4), the modal fluid force coefficients, Eq. (20), can be written as

$$p_n(t)=p_i^n(t)+M_n p_d^n(t)+M_n p_r^n(t), \tag{23}$$

where p_i^n denotes the projection of the incident pressure on the normal component of the nth eigenvector, namely

$$p_i^n(t)=\int_\Gamma \Phi_n^\zeta(\mathbf{x})p_i(\mathbf{x},t)\,\mathrm{dS_x}. \tag{24}$$

The last two terms of the right-hand side of Eq. (23) must now be expressed as a function of the given incident velocity and shell displacements. For this purpose, it is first useful to introduce the modal decomposition of the normal velocity induced by the incident wave:

$$\begin{pmatrix}0\\ \mathbf{v_i}(\mathbf{x},t)\mathbf{n_x}\end{pmatrix}=\sum_m v_i^m(t)\mathbf{\Phi_m}(\mathbf{x}),\quad v_i^m(t)=\frac{1}{M_m}\int_\Gamma \Phi_m^\zeta(\mathbf{x})\mathbf{v_i}(\mathbf{x},t)\mathbf{n_x}\,\mathrm{dS_x}. \tag{25}$$

Then substituting the normal components of the modal decompositions of both the incident normal velocity, Eq. (25), and the shell displacements, Eq. (2), into the boundary condition equation (19) yields

$$\frac{\partial p_d}{\partial \mathbf{n_x}}(\mathbf{x},t)=\sum_m \dot v_i^m(t)\Phi_m^\zeta(\mathbf{x}),\quad \frac{\partial p_r}{\partial \mathbf{n_x}}(\mathbf{x},t)=-\sum_m \ddot d_m(t)\Phi_m^\zeta(\mathbf{x}). \tag{26}$$

Owing to the acoustic problem linearity, the diffracted and radiated pressures are, respectively, sought in the form

$$p_d(\mathbf{x},t)=\sum_m p_{d,m}(\mathbf{x},t),\quad p_r(\mathbf{x},t)=\sum_m p_{r,m}(\mathbf{x},t), \tag{27}$$

so that each term of the above right-hand sides satisfies a unique component of the full boundary conditions, Eq. (26):

$$\frac{\partial p_{d,m}}{\partial \mathbf{n_x}}(\mathbf{x},t)=\dot v_i^m(t)\Phi_m^\zeta(\mathbf{x}),\quad \frac{\partial p_{r,m}}{\partial \mathbf{n_x}}(\mathbf{x},t)=-\ddot d_m(t)\Phi_m^\zeta(\mathbf{x}). \tag{28}$$

Note that only the m th eigenfunction appears in the right-hand sides of the above boundary conditions. However, the influence of all the shell modes are contained implicitly in the terms $p_{d,m}$ and $p_{r,m}$ due to the fluid coupling. By turning Eq. (28) into the Laplace domain, and by analogy with the general solution, Eq. (18), the Laplace transforms of the terms $p_{d,m}$ and $p_{r,m}$ can be written in the form

$$\hat p_{d,m}(\mathbf{x},s)=-s\hat v_i^m(s)\hat\Pi(\mathbf{x},s)\Phi_m^\zeta(\mathbf{x}), \tag{29}$$

$$\hat p_{r,m}(\mathbf{x},s)=s^2\hat d_m(s)\hat\Pi(\mathbf{x},s)\Phi_m^\zeta(\mathbf{x}), \tag{30}$$

where it is assumed that at $t=0$ the incident wave has not reached the submerged body yet, and that the shell is initially at rest. Note that the quantities $p_d^n(t)$ and $p_r^n(t)$, required for the evaluation of the modal fluid force coefficient $p_n(t)$, Eq. (23), represent, respectively, the diffracted and radiated pressures influence on the n th shell mode. As for the above terms, $p_{d,m}(\mathbf{x},t)$ and $p_{r,m}(\mathbf{x},t)$, they denote the pressure generated by the m th component of the diffracted and radiated pressure, respectively, and experienced by all the shell modes. Therefore, the first step towards the formulation of $p_d^n(t)$ and $p_r^n(t)$ consists in extracting the pressure components, on each structural mode, implicitly contains in $p_{d,m}(\mathbf{x},t)$ and $p_{r,m}(\mathbf{x},t)$. This can be achieved with the relation equations (21) and (22). Hence, the n th components of the diffracted and radiated pressure modal coefficients, denoted by $p_{d,m}^n(t)$ and $p_{r,m}^n(t)$, and generated by the m th modes of, respectively, the incident velocity and the shell displacement, take the form

$$\hat p_{d,m}^n(s)=-s\hat v_i^m(s)\frac{1}{M_n}\int_\Gamma \Phi_n^\zeta(\mathbf{x})\hat\Pi(\mathbf{x},s)\Phi_m^\zeta(\mathbf{x})\,\mathrm{dS_x}, \tag{31}$$

$$\hat p_{r,m}^n(s)=s^2\hat d_m(s)\frac{1}{M_n}\int_\Gamma \Phi_n^\zeta(\mathbf{x})\hat\Pi(\mathbf{x},s)\Phi_m^\zeta(\mathbf{x})\,\mathrm{dS_x}. \tag{32}$$

It is convenient to introduce the complex transfer function, $\hat Z_{n,m}(s)$, such that

$$\hat Z_{n,m}(s)=\int_\Gamma \Phi_n^\zeta(\mathbf{x})\hat\Pi(\mathbf{x},s)\Phi_m^\zeta(\mathbf{x})\,\mathrm{dS_x}. \tag{33}$$

In the Laplace domain, $\hat{Z}_{n,m}$ quantifies the link between the n th and m th shell eigenfunctions, arising from the fluid presence. The terms $p_d^n(t)$ and $p_r^n(t)$ are finally obtained by summing the contribution of all the incident velocity and shell displacement modes, respectively:

$$\hat{p}_d^n(s) = \sum_m \hat{p}_{d,m}^n(s) = -\frac{1}{M_n}\sum_m \hat{Z}_{n,m}(s) s \hat{v}_i^m(s), \tag{34}$$

$$\hat{p}_r^n(s) = \sum_m \hat{p}_{r,m}^n(s) = \frac{1}{M_n}\sum_m \hat{Z}_{n,m}(s) s^2 \hat{d}_m(s). \tag{35}$$

The modal fluid force coefficients, Eq. (23), are therefore fully determined in the Laplace domain by

$$\hat{p}_n(s) = \hat{p}_i^n(s) - \sum_m \hat{Z}_{n,m}(s) s \hat{v}_i^m(s) + \sum_m \hat{Z}_{n,m}(s) s^2 \hat{d}_m(s). \tag{36}$$

It appears that all the structural modes are involved in the n th modal fluid force coefficient. The modal equations, given by Eq. (5), are hence coupled by the fluid. The above expression, Eq. (36), holds for all two-dimensional thin shells whose boundary surface is regular, even if the method of separation of variables for the fluid cannot be used.

From the numerical computation point of view, the evaluation of the transfer functions $\hat{Z}_{m,n}(s)$, Eq. (33), is the most time-consuming part of the method. Firstly, the integral operators, $\hat{S}(\mathbf{x}, s)$ and $\hat{D}(\mathbf{x}, s)$, must be computed with a boundary element method for each point of the Laplace variable. Then the quantity $\hat{\Pi}(\mathbf{x}, s)$ is evaluated with a simple matrix inversion, Eq. (18), once again for each point of the Laplace vector. Each matrix to invert is full and of size N^2, with N denoting the boundary element number. However, the calculations of $\hat{S}(\mathbf{x}, s)$, $\hat{D}(\mathbf{x}, s)$ and the matrix inversion equation (18) are independent for each required value of s, which makes their numerical evaluations suitable to parallel processing.

The matrix $\hat{\Pi}(\mathbf{x}, s)$ is moreover independent on the structural modes and has to be evaluated only once. Since it depends only on the wetted surface geometry, it can be used for different materials and shell widths, which is particularly versatile. Once this matrix is evaluated, the transfer functions, Eq. (33), rapidly follow from simple multiplications and surface integrations. Their numerical evaluations can also be achieved thanks to parallel processing, since they are uncoupled.

If necessary, the modal fluid force coefficients can be expressed in the temporal domain by applying the convolution theorem to Eq. (36), which yields

$$p_n(t) = p_i^n(t) - \sum_m \int_0^t Z_{n,m}(t-\tau)\dot{v}_i^m(\tau)\,\mathrm{d}\tau + \sum_m \int_0^t Z_{n,m}(t-\tau)\ddot{d}_m(\tau)\,\mathrm{d}\tau. \tag{37}$$

The kernels, $Z_{n,m}(t)$, also called response functions, denote the fluid influence on the n th shell modes, induced by an impulsional motion of the m th modes. The convolution products reflect that the response is not instantaneous and involves acoustic wave propagation phenomena in the fluid domain. As expected, the diffracted pressure influence is expressed in terms of the response functions and the modal coefficients of the incident normal velocity. As for the radiated pressure influence, it involves the same response functions and the modal shell displacements coefficients, and is therefore the only pressure component coupled with the shell elasticity.

4. Resolution method for the fluid–structure interaction problem

Once the modal fluid force coefficients are put into the form of Eq. (37), the fluid–structure interaction problem can be easily solved. The substitution of Eq. (37) into each modal equation (5) yields an infinite number of fully coupled integro-differential equations. After truncation to a finite number of modes, N, the resulting system could be solved by a time-marching scheme. However, its linearity suggests the Laplace transform use to turn it into a simple algebraic matrix system, for each point of the Laplace variable:

$$\hat{\mathbf{M}}(s)\hat{\mathbf{d}}(s) = \mathcal{K}\hat{\mathbf{f}}(s) + \mathcal{K}\hat{\mathbf{Z}}(s) s \hat{\mathbf{v}}(s), \tag{38}$$

where the matrices $\hat{\mathbf{M}}(s)$ and $\hat{\mathbf{Z}}(s)$ are defined such that $\hat{\mathbf{M}}_{mn}(s) = s^2\mathcal{K}\hat{Z}_{n,m}(s)$ for $m \neq n$, $\hat{\mathbf{M}}_{nn}(s) = s^2\left(M_n + \mathcal{K}\hat{Z}_{n,n}(s)\right) + K_n$, and $\hat{\mathbf{Z}}_{mn}(s) = \hat{Z}_{m,n}(s)$, for all n and m in $[1; N]$. As for the vectors $\hat{\mathbf{d}}(s)$, $\hat{\mathbf{f}}(s)$, and $\hat{\mathbf{v}}(s)$, their components are, respectively, given by $\hat{\mathbf{d}}_n(s) = \hat{d}_n(s)$, $\hat{\mathbf{f}}_n(s) = \hat{f}_n(s) - \hat{p}_i^n(s)$, and $\hat{\mathbf{v}}_n(s) = \hat{v}_i^n(s)$, for all n in $[1; N]$. The modal displacement coefficients, contained in the vector $\hat{\mathbf{d}}(s)$, are therefore obtained in the Laplace domain through simple numerical matrix inversions, with the Laplace variable s as a parameter,

$$\hat{\mathbf{d}}(s) = \mathcal{K}[\hat{\mathbf{M}}(s)]^{-1}\hat{\mathbf{f}}(s) + \mathcal{K}[\hat{\mathbf{M}}(s)]^{-1}\hat{\mathbf{Z}}(s) s \hat{\mathbf{v}}(s). \tag{39}$$

The time-dependent modal displacement coefficients are then expressed in the time domain with a numerical inverse Laplace transform. This operation is carried out by an FFT-based algorithm together with a quotient-difference algorithm to accelerate the FFT series convergence and thus enhance solution accuracy [51,52]. This direct approach is useful when the given mechanical excitation, incident pressure, and incident normal velocity can be explicitly expressed in the Laplace domain, as in the following section example. If their expressions are known in the temporal domain only and neither

analytical nor numerical Laplace transforms are performed, an alternative is still possible by applying the convolution theorem to Eq. (39), which yields

$$\mathbf{d}(t) = \mathcal{K}\int_0^t \mathcal{L}^{-1}([\hat{\mathbf{M}}(s)]^{-1})(t-\tau)\mathbf{f}(\tau)\,\mathrm{d}\tau + \mathcal{K}\int_0^t \mathcal{L}^{-1}([\hat{\mathbf{M}}(s)]^{-1}\hat{\mathbf{Z}}(s))(t-\tau)\dot{\mathbf{v}}(\tau)\,\mathrm{d}\tau, \tag{40}$$

where $\mathcal{L}^{-1}(.)(t)$ denotes the Laplace transform inversion. The matrices resulting from this operation contain the response functions of the whole interaction problem, involving the shell elasticity, the modes coupling by the fluid presence and the acoustic waves influence. From a numerical computation point of view, this method is more time-consuming than the direct numerical Laplace transform inversion of the modal displacement coefficients, Eq. (39), since the inversion of the matrix $\hat{\mathbf{M}}(s)$ has first to be fully realized, then the numerical Laplace inversion of each of the matrix components performed, and finally matrix–vector convolution products achieved. Once the time-dependent modal displacement coefficients are obtained with one of the two aforementioned methods, the shell displacement field is directly obtained by the modal recomposition, Eq. (2).

5. Method illustration for the weak shock wave/circular thin shell interaction problem

The general method is here applied to the particular case of a two-dimensional circular evacuated thin shell of constant thickness h and radius R, submerged in an infinite fluid medium and subjected to a weak shock wave. A schematic of the problem is shown in Fig. 2. Since this case is well documented in the scientific literature, see for instance [13] and the references therein, it is well suited for the present approach validation.

5.1. Structural dynamics

Normalizing the variables according to Table 1, the shell equations take obviously the same form as Eq. (1), without mechanical excitations, and with the shell displacements given by $\mathbf{X}(\theta,t) = (U_\theta(\theta,t), U_r(\theta,t))^{\mathrm{T}}$. By taking into account the bending stiffness, the partial differential operator $[L]$ can be explicitly written as [44,45]

$$[L] = \mathcal{C}^2\begin{bmatrix} -(1+\lambda^2)\dfrac{\partial^2}{\partial\theta^2} & -\left(\dfrac{\partial}{\partial\theta} - \lambda^2\dfrac{\partial^3}{\partial\theta^3}\right) \\ \dfrac{\partial}{\partial\theta} - \lambda^2\dfrac{\partial^3}{\partial\theta^3} & 1+\lambda^2\dfrac{\partial^4}{\partial\theta^4} \end{bmatrix}, \tag{41}$$

where the dimensionless numbers $\mathcal{C}$ and λ are, respectively, defined by $\mathcal{C} = c_s/c_f$ and $\lambda^2 = h^2/(12R^2)$. The quantity c_s denotes the longitudinal speed of sound in the shell given by $c_s = \sqrt{E/(\rho_s(1-\nu^2))}$, with ρ_s, E, and ν, respectively, the shell density, Young's modulus, and Poisson's ratio. The *in vacuo* modal decomposition of the shell displacement can be easily obtained with a semi-analytical approach, due to the periodicity along θ. For this purpose, the shell displacement is sought in the form $\sum_{n=0}^{\infty}(U_n^\theta \sin(n\theta), U_n^r\cos(n\theta))^{\mathrm{T}}\mathrm{e}^{\mathrm{i}\Omega_n t}$. Its substitution into the shell equations without right-hand side yields, for each n, the following *in vacuo* eigenvalue/eigenvector problem:

$$\mathcal{C}^2\begin{bmatrix} (1+\lambda^2)n^2 & (1+\lambda^2 n^2)n \\ (1+\lambda^2 n^2)n & (1+\lambda^2 n^4) \end{bmatrix}\begin{pmatrix} U_n^\theta \\ U_n^r \end{pmatrix} = \Omega_n^2\begin{pmatrix} U_n^\theta \\ U_n^r \end{pmatrix}. \tag{42}$$

This problem is then solved with a classical Arnoldi method [53]. For each n, two eigenpairs are admitted, corresponding to the two branches of the spectrum: the first branch, denoted by $p=1$ in the following, is dominated by the shell bending, and the second one, denoted by $p=2$, is dominated by the shell traction [45]. For $n=0$, only the traction branch has a

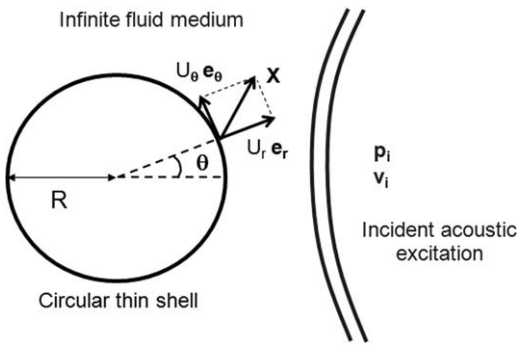

Fig. 2. Submerged two-dimensional circular thin shell subjected to an incident acoustic excitation.

physical meaning and corresponds to the breathing mode. The modal decomposition of the time-dependent displacement vector can therefore be written as

$$\mathbf{X}(\theta,t) = d_{02}(t)\mathbf{\Phi_{02}}(\theta) + \sum_{n=1}^{\infty}\sum_{p=1}^{2} d_{np}(t)\mathbf{\Phi_{np}}(\theta), \tag{43}$$

where the terms $d_{np}(t)$ are the time-dependent displacement coefficients corresponding to the p th branch of the n th Fourier mode, and the quantities $\mathbf{\Phi_{np}}(\theta)$ denote the corresponding eigenfunctions, whose components are defined in terms of the solutions of Eq. (42):

$$\mathbf{\Phi_{np}}(\theta) = \begin{pmatrix} \Phi^{\theta}_{np}(\theta) \\ \Phi^{r}_{np}(\theta) \end{pmatrix} = \begin{pmatrix} U^{\theta}_{np}\sin(n\theta) \\ U^{r}_{np}\cos(n\theta) \end{pmatrix}. \tag{44}$$

Therefore, the functions $\mathbf{\Phi_{np}}(\theta)$ satisfy both the eigenvalue problem $[L]\ \mathbf{\Phi_{np}}(\theta) = \Omega^2_{np}\mathbf{\Phi_{np}}(\theta)$, which is another formulation of Eq. (42), and the orthogonality property of the same form of Eq. (4).

The modal mass is here explicitly given by $M_{np} = 2\pi(U^r_{02})^2$ for n and p equal to 0 and 2, respectively, and $M_{np} = \pi[(U^{\theta}_{np})^2 + (U^r_{np})^2]$ for $n \geq 1$ and $p = 1$ or 2. The *in vacuo* circular eigenfunctions are now fully determined and the usual manipulations, recalled in Section 2, lead to the modal equations governing the shell dynamics:

$$M_{np}\ddot{d}_{np}(t) + K_{np}d_{np}(t) = -\mathcal{K}p_{np}(t), \tag{45}$$

with the modal stiffness K_{np} defined here by $K_{np} = \Omega^2_{np}M_{np}$, and the modal fluid force coefficient p_{np} given by

$$p_{np}(t) = \int_0^{2\pi} \mathbf{\Phi}^{\mathrm{T}}_{\mathbf{np}}(\theta)\mathbf{p}(\theta,t)\,\mathrm{d}\theta. \tag{46}$$

These coefficients are still to be explicitly expressed to solve the modal equations.

5.2. The modal fluid force coefficients

The fluid loading formulation, Eq. (36), can be simplified for the particular case of a circular thin shell submerged in an infinite fluid medium. Contrary to the general case, the geometrical revolution symmetry induces here a decoupling of the Fourier modes. Finally, by taking explicitly into account the periodicity along θ and following the general method of Section 3.2, it is easily shown that only the two branches of a Fourier mode are coupled by the fluid presence. The fluid force coefficients take therefore the form

$$\hat{p}_{np}(s) = \hat{p}^{np}_i(s) - \sum_{q=1}^{2}\hat{Z}^n_{p,q}(s)s\hat{v}^{nq}_i(s) + \sum_{q=1}^{2}\hat{Z}^n_{p,q}(s)s^2\hat{d}_{nq}(s). \tag{47}$$

The complex transfer functions, $\hat{Z}^n_{p,q}(s)$ represent the fluid loading induced by the impulsional solicitation of the q th branch of the n th Fourier mode, on the p th branch. They can be explicitly written in the Laplace domain as

$$\hat{Z}^n_{p,q}(s) = \int_0^{2\pi} \Phi^r_{np}(\theta)\hat{A}(\theta,s)\Phi^r_{nq}(\theta)\,\mathrm{d}\theta. \tag{48}$$

At this step, it is possible to check the method validity with the response functions obtained analytically for instance by Iakovlev [13] and defined in the Laplace domain by

$$\hat{Z}_n(s) = -\frac{K_n(s)}{sK'_n(s)}. \tag{49}$$

It is easily shown that the present formulation and the analytical one are linked with the following relation:

$$\hat{Z}_n(s) = \frac{1}{\pi}\sum_{p=1}^{2}\frac{1}{(U^{\theta}_{np})^2 + (U^r_{np})^2}\hat{Z}^n_{p,p}(s). \tag{50}$$

The left-hand side term corresponds to the fluid loading induced by the impulsional solicitation of the n th Fourier shell mode. The right-hand side results from the complex transfer function combination $\hat{Z}^n_{p,p}(s)$ for a fixed n. The comparison between their inverse Laplace transforms performed numerically provides a way to evaluate the numerical computation of the integral operator $\hat{A}(\theta,s)$.

Figs. 3 and 4 compare the analytical and numerical calculations of response functions in the temporal domain (i.e. the Laplace inverse of $\hat{Z}_n(s)$) for $n = 2$ and 80. Numerical calculation are performed with BEM discretization, using 1000 boundary elements; as for the time sampling, 512 calculation points are used in the interval $[0, T^*]$, with $T^* = 5$. Constant and linear schemes are used for the numerical calculation of the integrals and yield identical results in the present case.

Numerical calculation of the $\hat{Z}^n_{p,q}(s)$ for each n, p, q, and s is performed with a BEM method using CHIEF points [42] in order to tackle the spurious frequency problem. Fig. 5 compares the BEM calculation with and without CHIEF points to the

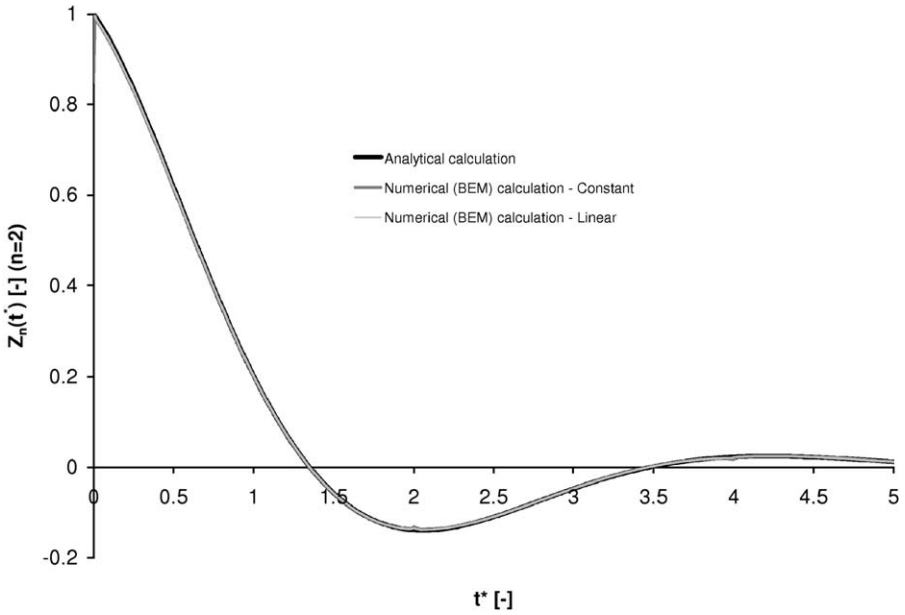

Fig. 3. Comparison of the analytical and computed response functions in the temporal domain for $n = 2$.

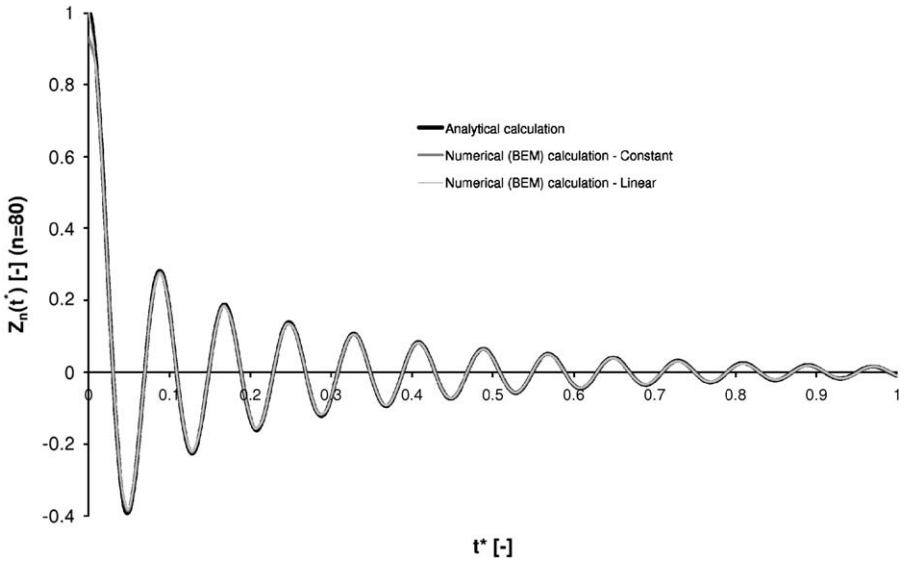

Fig. 4. Comparison of the analytical and computed response functions in the temporal domain for $n = 80$.

analytical expression of $\hat{Z}_n(s^*)$ (with $s^* = sR/c_f$ being the non-dimensional Laplace variable) in the Laplace domain and highlights the numerical treatment of the spurious frequencies.

5.3. Resolution of the fluid–structure interaction problem

Substituting the fluid loading expression, Eq. (47) in the modal equation, Eq. (45), and turning the resulting system in the Laplace domain, yield for each n th Fourier modes, the algebraic matrix equation:

$$\hat{\mathbf{M}}_n(s)\hat{\mathbf{d}}_n(s) = \mathcal{K}\hat{\mathbf{f}}_n(s) + \mathcal{K}\hat{\mathbf{Z}}_n(s)s\hat{\mathbf{v}}_n(s), \tag{51}$$

where the matrices $\hat{\mathbf{M}}_n(s)$ and $\hat{\mathbf{Z}}_n(s)$ are defined such that $\hat{\mathbf{M}}_{\mathbf{n}pq}(s) = s^2\mathcal{K}\hat{Z}^n_{p,q}(s)$ for $p \neq q$, $\hat{\mathbf{M}}_{\mathbf{n}pp}(s) = s^2(M_{np} + \mathcal{K}\hat{Z}^n_{p,p}(s)) + K_{np}$, and $\hat{\mathbf{Z}}_{\mathbf{n}pq}(s) = \hat{Z}^n_{p,q}(s)$, for p and q in $[1;2]$. As for the vectors $\hat{\mathbf{d}}_n(s)$, $\hat{\mathbf{f}}_n(s)$, and $\hat{\mathbf{v}}_n(s)$, their components are, respectively, given by

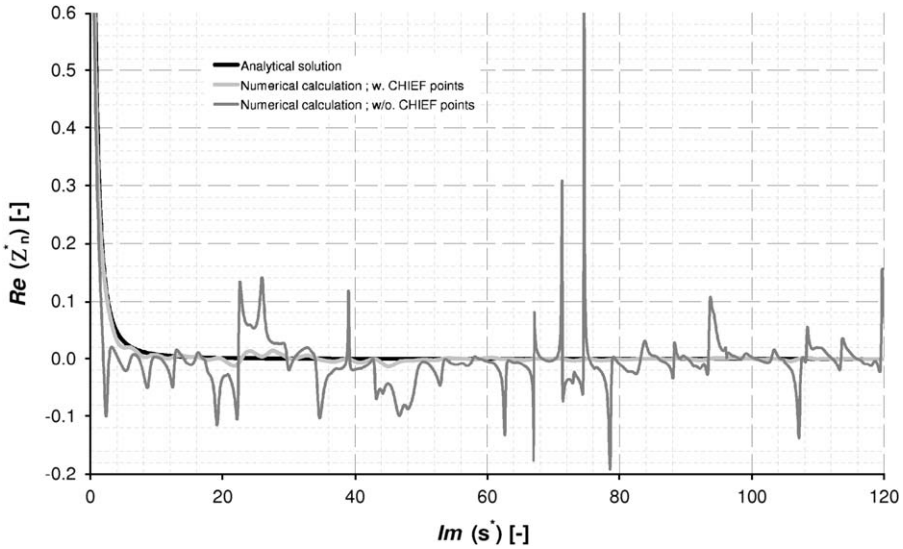

Fig. 5. Computation of a modal response function with a BEM method with and without CHIEF points.

$\hat{\mathbf{d}}_{\mathbf{n}p}(s) = \hat{d}_{np}(s)$, $\hat{\mathbf{f}}_{\mathbf{n}p}(s) = -\hat{p}_i^{np}(s)$, and $\hat{\mathbf{v}}_{\mathbf{n}p}(s) = \hat{v}_i^{np}(s)$, for all $p = 1, 2$. As described in Section 4, the modal displacement coefficients in the Laplace domain are therefore obtained through simple numerical matrix inversions, with the only difference that the Fourier modes are here not coupled and the matrices to invert are of size 2×2. Then the shell displacement field is derived by the numerical inversion of the modal displacement coefficient Laplace transform, and the modal recomposition, Eq. (43).

Eq. (51) is the governing equation for the immersed shell dynamics when subjected to an incoming pressure loading, which is described by the incident pressure term and by the diffracted pressure term: the former is given by the incident pressure wave ($-\hat{p}_i^{np}(s)$), while the latter is related to the incident velocity wave ($\hat{v}_i^{np}(s)$). In the present case, the incident pressure wave and its corresponding velocity field are computed according to the analytical model proposed by Cole [54]; the incoming pressure loading is described as an exponentially decaying function:

$$P(t) = \Pi \exp(-t/\tau), \tag{52}$$

with Π and τ given by the following correlations:

$$\Pi = \Pi_0 \left(\frac{C^a}{D}\right)^b, \quad \tau = \tau_0 C^a \left(\frac{C^a}{D}\right)^c,$$

where C stands for the mass of explosive and D is the standoff point, a, b, and c depend on the type of explosive [54].

Implementation of the imposed pressure p^i and velocity v^i in the Laplace domain poses no particular difficulty and is beyond the scope of the present paper; the methodology adopted in the present case is very similar to what is proposed by Iakovlev [12], which could be referred to for further details on the matter.

An application example is proposed with the following characteristics: $R = 1$, $h = 0.1\,\text{m}$, $\rho_s = 7800\,\text{kg/m}^3$, $E = 2.1 \times 10^{11}\,\text{Pa}$, $\nu = 0.3$, $\rho_f = 1000\,\text{kg/m}^3$, $c = 1500\,\text{m/s}$, $C = 1\,\text{kg}$, $D = 5\,\text{m}$. Fig. 6 features the computed displacement field (radial component $u_r(\theta, t)$) at various locations on the shell circumference ($\theta = 0, \pi/4, \pi/3, 3\pi/4$, and π) and compares the numerical simulation with a reference analytical solution (as presented for instance in [55]).

Calculation is performed with some 90 boundary elements and yields a qualitative good agreement with the analytical solution in the proposed two-dimensional case under consideration.

5.4. On the efficiency and versatility of the proposed method

BEM calculation of the modal response functions of the submerged structure is a conspicuous feature of the proposed method which makes it versatile and promising in the industrial context.

On the one hand, BEM-based calculation allows for a dramatic computational cost reduction as it only requires the mesh of the wetted surface; in comparison FEM-based calculation requires the modeling and meshing of a significant part of the fluid surrounding the submerged structure. Fig. 7 gives an example of an FEM-based calculation for a circular elastic shell immersed within a fluid and subjected to an acoustic pulse, i.e. in the same configuration as described in Fig. 2, but with different parameters. Calculation is performed with the ABAQUS finite element code, assuming a plane wave propagation of

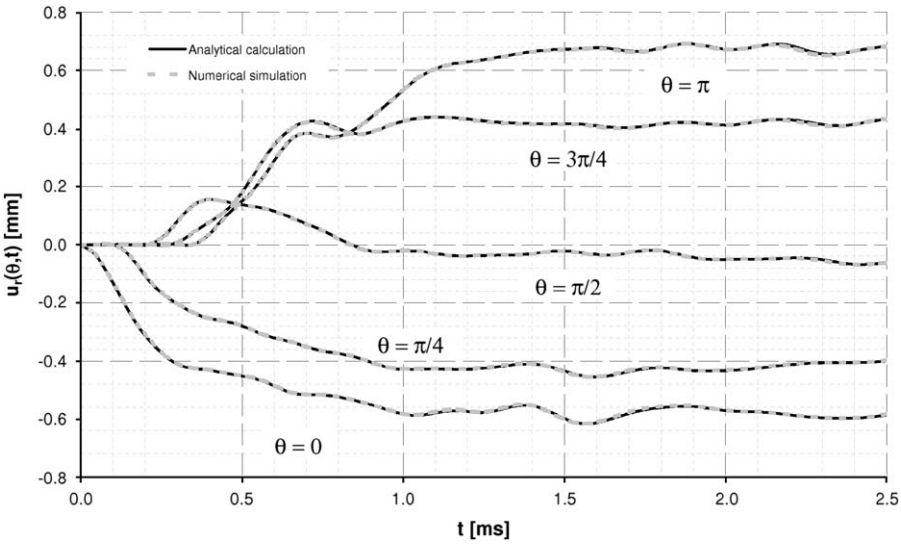

Fig. 6. Submerged shell subjected to a pressure loading: comparison of numerical and analytical calculation.

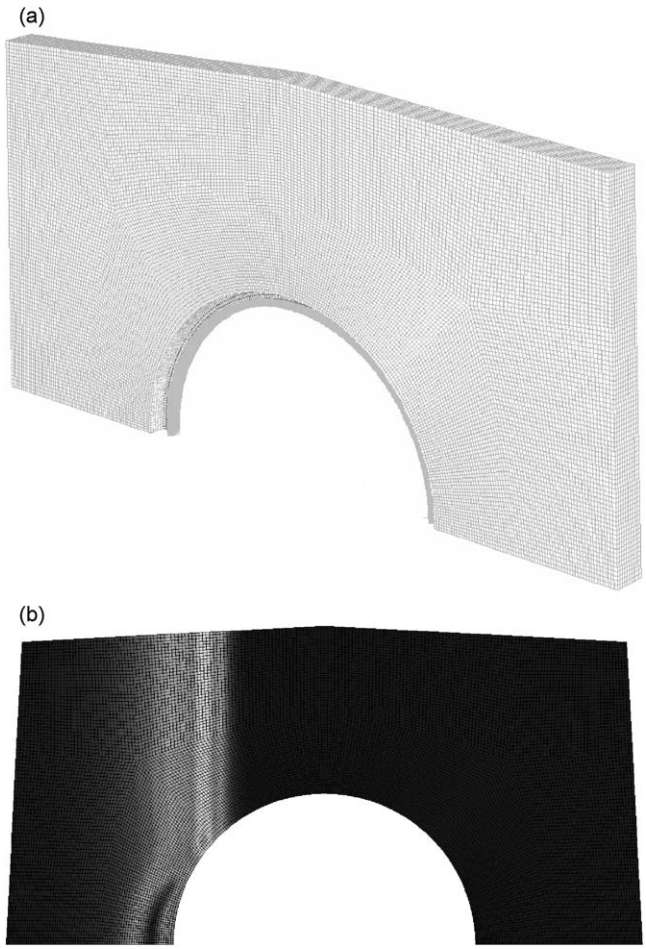

Fig. 7. FEM calculation of the dynamic response of a submerged circular shell subjected to an acoustic pulse.

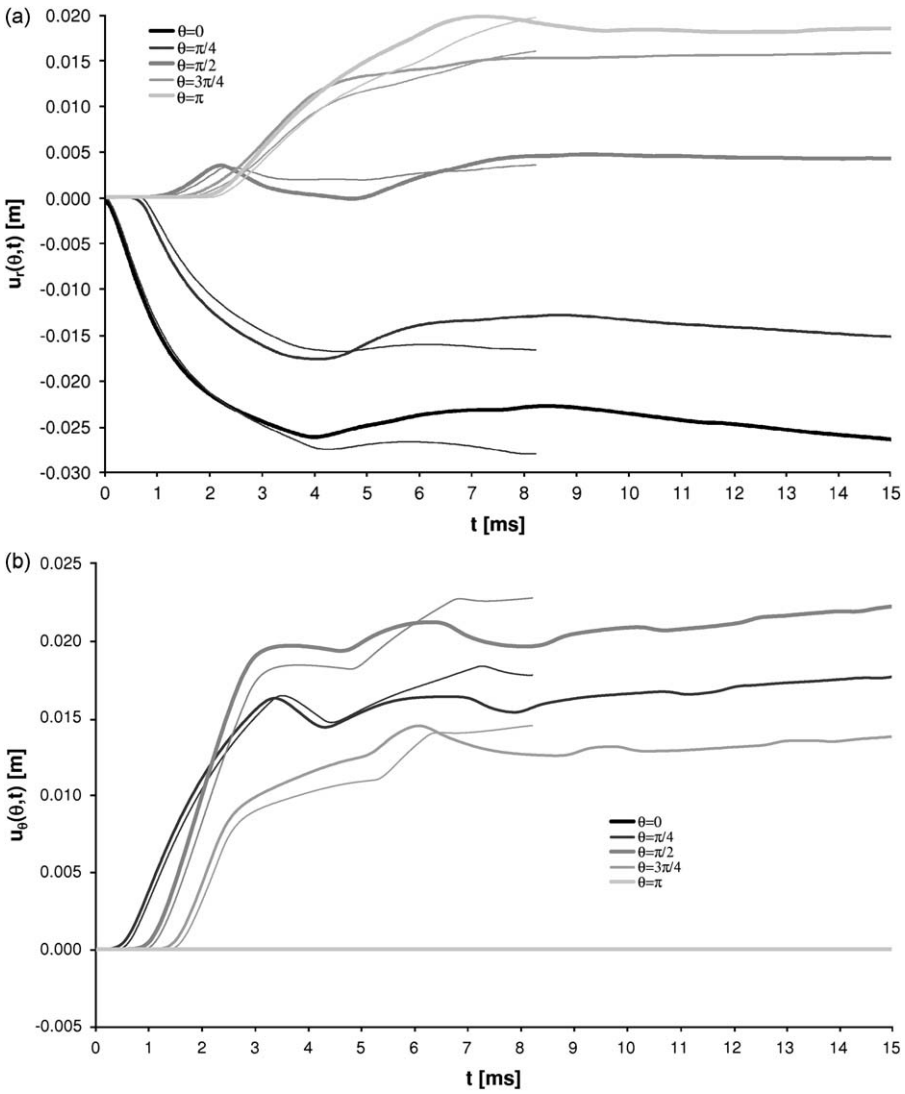

Fig. 8. Radial and ortho-radial displacement of a submerged shell subjected to an acoustic pulse with FEM calculation (thick curves) and with the proposed method (thin curves).

the acoustic pulse; such finite element calculation is representative of what can be performed for design and/or pre-design purposes with industrial numerical tools.

Fig. 8 gives the time history of the computed radial and ortho-radial displacements at $\theta = 0, \pi/4, \pi/2, 2\pi/4$, and π: finite element computation with the ABAQUS code and BEM-based response function computation with the MATLAB code are compared.[1]

Since the two simulations are carried out with different numerical tools, one can only draw some qualitative conclusions as for computational cost. For the sake of illustration, it is however worth noting the computational effort with both approaches. With the MATLAB code developed for the present study, a single computation of the shell response (including the evaluation of the eigenmodes and the calculation of the response function) can be run within an hour, while a single FEM calculation can be run overnight with the ABAQUS code on a standard PC, with no particular difficulty. Although affordable for industrial application, such computational cost can become prohibitive when one wishes to perform numerous calculations, for instance when trying to estimate the influence of a given design parameter on the global behavior of the system under concern. BEM-based oriented simulations can be employed for industrial purposes, but they also tend to be very costly and cannot be used for systematic and repetitive calculations.

[1] In the simulation presented in the previous subsection, the acoustic pulse was assumed to propagate as a circular wave; in the ABAQUS simulation a plane wave propagation is assumed: therefore, the finite element simulation and the BEM-based with response function simulation are not expected to yield an identical result. However, as conveyed by Fig. 8, there is a good qualitative agreement between the two simulations.

On the other hand, proposing a response-function oriented approach as in the present case allows for systematic computation since once the response functions have been determined, numerous calculations can be rapidly performed while changing the problem parameters. More precisely, the numerical evaluation of the quantity $\hat{\Pi}(\mathbf{x}, s)$, defined in Eq. (18), is the most time-consuming part of the method, but it depends only on the wetted surface geometry and can be used for different materials and shell widths. Once this matrix is evaluated, the transfer functions, Eq. (33), can be rapidly computed. They involve the numerical evaluation of the system eigenmodes and therefore depend on the shell width and material. They nevertheless remain independent on an internal or external loading.

In the case depicted in Fig. 2 for instance, the influence of the shell thickness h or the explosion distance D (which only influence the loading pressure) can be estimated with straightforward calculations, see Figs. 9 and 10. Once the quantity $\hat{\Pi}(\mathbf{x}, s)$ and the response functions are computed, the response of the structure can be calculated in a short period of time: for the sake of illustration, the previous calculation have been performed with a dedicated MATLAB tool. While the first

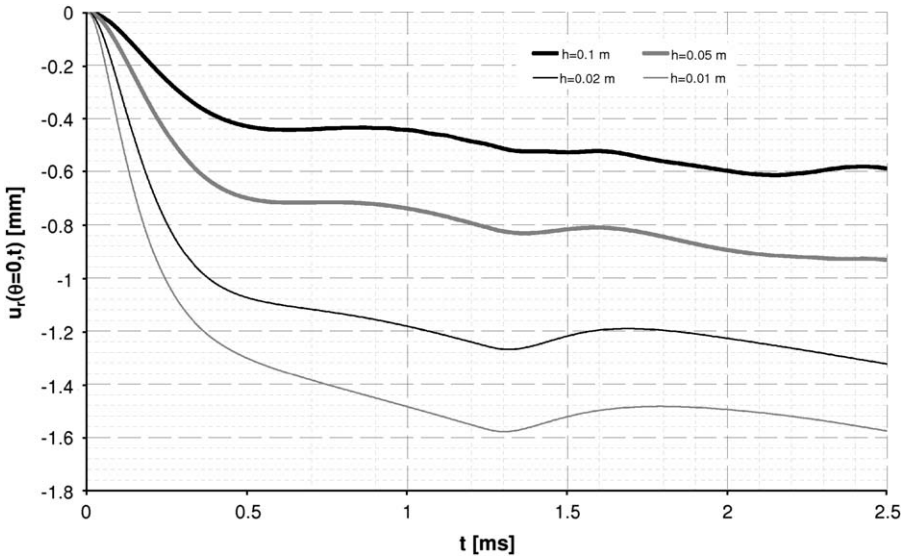

Fig. 9. Influence of the shell thickness: the first simulation involves the determination of the quantity $\hat{\Pi}(\mathbf{x}, s)$, the system eigenmodes and the response functions; the following simulations only require the determination of the system eigenmodes and the response functions; the shock response follows from straightforward calculations with the previously computed quantity $\hat{\Pi}(\mathbf{x}, s)$.

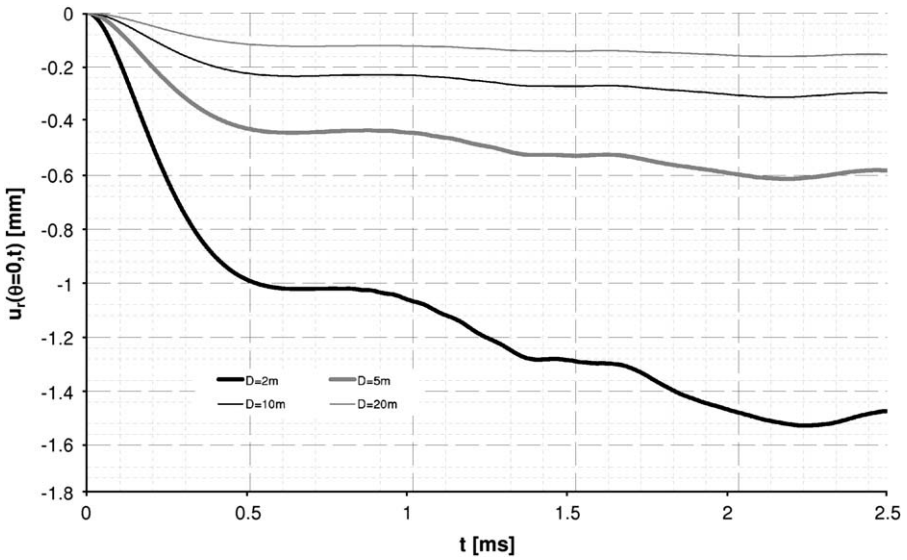

Fig. 10. Influence of the explosion distance: the first simulation involves the determination of the quantity $\hat{\Pi}(\mathbf{x}, s)$, the system eigenmodes and the calculation of the response functions; the shock response for the following simulations come from straightforward calculations with the previously computed response functions, only the analytical calculation of the pressure pulse is varied.

calculation of each series require some 30 min in order to compute the response functions, each subsequent individual calculation only require 3 min, using the previously computed response functions. In a "complete" FEM or BEM-based calculation, any change on those parameters would require a specific run with appreciatively the same computational cost.

6. Conclusion

In the present paper, a numerical method for the interaction between a submerged shell and an acoustic pressure pulse has been proposed for application to the pre-design or the design of naval structures subjected to underwater explosions. The method is based on a classical modal reduction technique for the structure sub-problem together with a dimensional reduction of the fluid sub-problem with a BEM discretization of the acoustic wave propagation.

It therefore provides a versatile and robust approach, which is well suited for industrial application since it is based on the evaluation of response functions which can be used in various configurations without performing additional calculation. The proposed method is also designed in order to be applicable to parallel processing, which makes it efficient enough to be used for design purposes.

The underlying principle of the method is formulated in a general case and applied in a particular validation example, namely in the case of a two-dimensional elastic submerged shell subjected to a pressure loading which is representative of an underwater explosion; as a conspicuous feature of the proposed method, a qualitative agreement between analytical and numerical calculation is highlighted. Efficiency of the so-called "CHIEF points method" associated to the BEM approach is also reported in the application example to tackle the "spurious frequency" problem in the resolution of the fluid pressure field.

Possible extensions of the method are under study for instance in order to turn to three-dimensional problems; reduction techniques such as POD or eigenmodes basis are also considered to deal with a nonlinear description of the structure dynamics, together with BEM coupling for the fluid pressure loading. Further investigation on the shell dynamic modeling (thin/thick shell models) will be presented in related publications.

Acknowledgments

The first author gratefully acknowledges the financial support provided by DCNS Group when he was a PhD student. The authors also thank Younes Souaidi and Gilles Serre, both mechanical and mathematical engineering students, for their dedicated assistance on the numerical computation of the method.

References

[1] G.I. Taylor, *The Pressure and Impulse of Submarine Explosion Waves on Plate*, Cambridge University Press, Cambridge, 1941.
[2] A.H. Keil, The response of ships to underwater explosions, *Transactions Society of Naval Architects and Marine Engineers* (1961) 366–410.
[3] G.J. O'Hara, P.F. Cunnif, Scaling for shock response of equipment in different submarines, *Shock and Vibration Bulletin* 1 (1993) 161–170.
[4] C. Leblond, J.-F. Sigrist, B. Auvity, H. Peerhossaini, A semi-analytical approach to the study of an elastic circular cylinder confined in a cylindrical fluid domain subjected to small-amplitude transient motions, *Journal of Fluids and Structures* 25 (2009) 134–154.
[5] H. Huang, An exact analysis of the transient interaction of acoustic plane waves with a cylindrical elastic shell, *Journal of Applied Mechanics* 37 (1970) 1091–1099.
[6] H. Huang, Y.F. Wang, Transient interaction of spherical acoustic waves and a cylindrical elastic shell, *Journal of the Acoustical Society of America* 48 (1970) 228–235.
[7] H. Huang, Y.F. Wang, Early-times interaction of spherical acoustic waves and a cylindrical elastic shell, *Journal of the Acoustical Society of America* 50 (1971) 885–891.
[8] H. Huang, Transient response of two fluid-coupled cylindrical elastic shells to an incident pressure pulse, *Journal of Applied Mechanics* 46 (1979) 513–518.
[9] S. Iakovlev, Interaction of a spherical shock wave and a submerged fluid-filled circular cylindrical shell, *Journal of Sound and Vibration* 255 (2002) 615–633.
[10] S. Iakovlev, Influence of a rigid coaxial core on the stress–strain state of a submerged fluid-filled circular cylindrical shell subjected to a shock wave, *Journal of Fluids and Structures* 19 (2004) 957–984.
[11] S. Iakovlev, External shock loading on a submerged fluid-filled cylindrical shell, *Journal of Fluids and Structures* 22 (2006) 997–1028.
[12] S. Iakovlev, Submerged fluid-filled cylindrical shell subjected to a shock wave: fluid–structure interaction effects, *Journal of Fluids and Structures* 23 (2007) 117–142.
[13] S. Iakovlev, Interaction between a submerged evacuated cylindrical shell and a shock wave—part I: diffraction-radiation analysis, *Journal of Fluids and Structures* 24 (2008) 1077–1097.
[14] S. Iakovlev, Interaction between a submerged evacuated cylindrical shell and a shock wave—part II: numerical aspects of the solution, *Journal of Fluids and Structures* 24 (2008) 1098–1119.
[15] H. Huang, H. Mair, Neoclassical solution of transient interaction of plane acoustic waves with a spherical elastic shell, *Shock and Vibration* 33 (1996) 85–98.
[16] M.A. Sprague, T.L. Geers, Response of empty and fluid-filled, submerged spherical shell to plane and spherical step-exponential acoustic waves, *Shock and Vibration* 6 (1999) 147–157.
[17] H.U. Mair, Benchmarks for submerged structure response to underwater explosion, *Shock and Vibration* 6 (1999) 169–181.
[18] H.U. Mair, Review: hydrocodes for structural response to underwater explosion, *Shock and Vibration* 6 (1999) 81–96.
[19] P. Pettes, *Infinite Elements*, Penshaw Press, 1992.
[20] I. Harari, R. Djellouli, Analytical study of the effect of wave number on the performance of local absorbing boundary conditions for acoustic scattering, *Applied Numerical Mathematics* 50 (2004) 15–47.
[21] C.A. Brebbia, J.C.F. Telles, L.C. Wrobel, *Boundary Element Techniques Theory and Applications in Engineering*, Springer, New York, 1983.
[22] D.E. Beskos, Boundary elements methods in dynamic analysis: part II (1986–1996), *Applied Mechanics Review* 50 (1997) 149–197.

[23] H. Huang, G.C. Everstine, W.F. Wang, Retarded potential techniques for the analysis of submerged structures impinged by weak shock waves, in: T. Belytschko, T.L. Geers (Eds.), *Computational Methods for Fluid–Structure Interaction Problems*, ASME, New York, 1977, pp. 83–93.
[24] P.H.L. Groenenboom, Solution of the retarded potential problem and numerical stability, in: C.A. Brebia (Ed.), *Boundary Element*, Springer, New York, 1984, pp. 57–74.
[25] A.M. Figueiredo, Differential-delay Equations of Advanced Type and Discretization of Kirchoffs Integral Equation, Ph.D. Dissertation, Boston University, Aerospace and Mechanical Engineering Department, 1992.
[26] C.T. Dyka, R.P. Ingel, Transient fluid–structure interaction in naval applications using the retarded potential method, *Engineering Analysis with Boundary Elements* 21 (1998) 245–251.
[27] C.A. Felippa, A family of early time approximations for fluid structure interaction, *Journal of Applied Mechanics* 47 (1980) 703–708.
[28] R.D. Mindlin, H.H. Bleich, Response of an elastic cylindrical shell to a transverse step shock wave, *Journal of Applied Mechanics* 20 (1953) 189–195.
[29] T.L. Geers, Residual potential and approximate methods for three-dimensional fluid–structure interaction problem, *Journal of the Acoustical Society of America* 49 (1971) 1505–1510.
[30] T.L. Geers, P. Zhang, Doubly asymptotic approximations for submerged structures with internal fluid volumes: formulation, *Journal of Applied Mechanics* 61 (1994) 893–899.
[31] T.L. Geers, P. Zhang, Doubly asymptotic approximations for submerged structures with internal fluid volumes: evaluation, *Journal of Applied Mechanics* 61 (1994) 900–906.
[32] T.L. Geers, Doubly asymptotic approximations for transient motions of submerged structures, *Journal of the Acoustical Society of America* 64 (1978) 1500–1508.
[33] J.A. De Runtz, C.C. Rankin, *Application of the USA and USA-STAGS Codes to Underwater Shock Problems*, Vols. 1 and 2, Palo Alta, CA, 1990.
[34] C.C. Liang, Y.S. Tai, Shock responses of a surface ship subjected to noncontact underwater explosions, *Ocean Engineering* 33 (2006) 748–772.
[35] K.C. Park, M. Lee, Y.-S. Park, New approximations of external acoustic–structural interactions, part I: model derivation, *ICSV13*, Vienna, Austria, July 2006, pp. 2–6.
[36] M. Lee, Y.-S. Park, K.C. Park, New approximations of external acoustic–structural interactions, part II: model evaluation, *ICSV13*, Vienna, Austria, July 2006, pp. 7–14.
[37] H. Huang, Y.F. Wang, Asymptotic fluid–structure interaction theories for acoustic radiation prediction, *Journal of the Acoustical Society of America* 77 (1985) 1389–1394.
[38] P.R. Stepanishen, Transient vibratory response of fluid-loaded structures using convolution integral equations, *Journal of the Acoustical Society of America* 101 (1997) 1877–1889.
[39] J.E. Chisum, Multimaterial Eulerian and Coupled Lagrangian–Eulerian Finite Element Analysis of Underwater Shock Problems, Ph.D. Dissertation, Naval Postgraduate School, Monterey, CA, 1995.
[40] D.J. Chappell, P.J. Harris, D. Henwood, R. Chakrabarti, A stable boundary element method for modeling transient acoustic radiation, *Journal of the Acoustical Society of America* 120 (2006) 74–80.
[41] A.J. Burton, G.F. Miller, The application of integral equation methods to the numerical solution of some exterior boundary-value problems, *Proceedings of the Royal Society of London, Serie A*, Vol. 323, 1971, pp. 201–210.
[42] T.W. Wu, *Boundary Element Acoustics*, WIT Press, 2000.
[43] A. Baillard, J. -M Conoir, D. Décultot, G. Maze, A. Klauson, J. Metsaveer, Acoustic scattering from fluid-loaded stiffened cylindrical shell: analysis using elasticity theory, *Journal of the Acoustical Society of America* 107 (2000) 3208–3216.
[44] A. Leissa, *Vibration of Shells*, Acoustical Society of America, New York, 1973.
[45] F. Axisa, *Modelling of Mechanical Systems*, *Vol. 2*, *Structural Elements*, Elsevier, Amsterdam, 2005.
[46] L.C. Wrobel, *The Boundary Element Method, Vol. 1: Application in Thermo-Fluids and Acoustics*, Wiley, New York, 2002.
[47] M. Costabel, Time-dependent problems with the boundary integral equation method, in: E. Stein, R. De Borst, T. Hughes (Eds.), *Encyclopedia of Computational Mechanics*, Wiley, New York, 2004 (Chapter 22).
[48] P.M. Morse, H. Feshbach, *Methods of Theoretical Physics*, McGraw-Hill, London, 1953.
[49] M. Bruneau, T. Scelo, *Fundamentals of Acoustics*, Iste Publishing Company, London, 2005.
[50] M. Abramowitz, I.A. Stegun, *Handbook of Mathematical Functions*, Dover, New York, 1970.
[51] L. Brancik, Utilization of quotient-difference algorithm in FFT based numerical ILT method, *Proceedings of the 11th Radioelektronica*, Brno, Czech Republic, 2001, pp. 352–355.
[52] L. Brancik, Utilization of Matlab in simulation of linear hybrid circuits, *Radioengineering* 12 (2003) 6–11.
[53] R.B. Lehoucq, D.C. Sorensen, Deflation techniques for an implicitly re-started Arnoldi iteration, *Journal on Matrix Analysis and Applications* 17 (1996) 789–821.
[54] R.H. Cole, *Underwater Explosions*, Princeton University Press, Princeton, NJ, 1948.
[55] J.F. Sigrist, Analytical and numerical study of the interaction of an acoustic shock wave and an immersed elastic structure. *Pressure Vessel and Piping*, Chicago, 27–31 July 2008.